Can classical Schwarz methods for time-harmonic elastic waves converge?

Romain Brunet, Victorita Dolean, and Martin J. Gander

1 Mathematical model

The propagation of waves in elastic media is a problem of undeniable practical importance in geophysics. In several important applications - e.g. seismic exploration or earthquake prediction - one seeks to infer unknown material properties of the earth's subsurface by sending seismic waves down and measuring the scattered field which comes back, implying the solution of inverse problems. In the process of solving the inverse problem (the so-called "full-waveform inversion") one needs to iteratively solve the forward scattering problem. In practice, each step is done by solving the appropriate wave equation using explicit time stepping. However in many applications the relevant signals are band-limited and it would be more efficient to solve in the frequency domain. For this reason we are interested here in the time-harmonic counterpart of the Navier or Navier-Cauchy equation (see [7, Chapter 5.1] or [11, Chapter 9][1]), which is a linear mathematical model for elastic waves

$$-\left(\Delta^e + \omega^2\rho\right)\mathbf{u} = \mathbf{f} \quad \text{in } \Omega, \quad \Delta^e\mathbf{u} = \mu\Delta\mathbf{u} + (\lambda+\mu)\nabla(\nabla\cdot\mathbf{u}), \tag{1}$$

where $\mathbf{u}$ is the displacement field, $\mathbf{f}$ is the source term, ρ is the density that we assume real, $\mu, \lambda \in [\mathbb{R}_+^*]^2$ are the Lamé coefficients, and ω is the time-harmonic frequency for which we are interested in the solution. An example of a discretization

Romain Brunet
Department of Mathematics and Statistics, University of Strathclyde, United Kingdom, e-mail: romain.brunet@strath.ac.uk

Victorita Dolean
Université Côte d'Azur, France, Department of Mathematics and Statistics, University of Strathclyde, United Kingdom, e-mail: victorita.dolean@strath.ac.uk

Martin J. Gander
Section des Mathématiques, Université de Genève, Switzerland, e-mail: martin.gander@unige.ch

[1] For the fascinating history on how Navier discovered the equation and then rapidly turned his attention to fluid dynamics, see [3].

of this equation was presented in [10]. In our case, we assumed small deformations which lead to linear equations and consider isotropic and homogeneous materials which implies that the physical coefficients are independent of the position and the direction. Due to their indefinite nature, the Navier equations in the frequency domain (1) are notoriously difficult to solve by iterative methods, especially if the frequency ω becomes large, similar to the Helmholtz equation [8], and there are further complications as we will see. We study here if the classical Schwarz method could be a candidate for solving the time harmonic Navier equations (1) iteratively.

2 Classical Schwarz Algorithm

To understand the convergence of the classical Schwarz algorithm applied to the time harmonic Navier equations (1), we study the equations on the domain $\Omega := \mathbb{R}^2$, and decompose it into two overlapping subdomains $\Omega_1 := (-\infty, \delta) \times \mathbb{R}$ and $\Omega_2 := (0, \infty) \times \mathbb{R}$, with overlap parameter $\delta \geq 0$. The classical parallel Schwarz algorithm computes for iteration index $n = 1, 2, \ldots$

$$\begin{aligned} -\left(\Delta^e + \omega^2\rho\right)\mathbf{u}_1^n &= \mathbf{f} && \text{in } \Omega_1,\\ \mathbf{u}_1^n &= \mathbf{u}_2^{n-1} && \text{on } x = \delta,\\ -\left(\Delta^e + \omega^2\rho\right)\mathbf{u}_2^n &= \mathbf{f} && \text{in } \Omega_2,\\ \mathbf{u}_2^n &= \mathbf{u}_1^{n-1} && \text{on } x = 0. \end{aligned} \tag{2}$$

We now study the convergence of the classical parallel Schwarz method (2) using a Fourier transform in the y direction. We denote by $k \in \mathbb{R}$ the Fourier variable and $\hat{\mathbf{u}}(x, k)$ the Fourier transformed solution,

$$\hat{\mathbf{u}}(x, k) = \int_{-\infty}^{\infty} \mathrm{e}^{-\mathrm{i}ky}\, \mathbf{u}(x, y)\, \mathrm{d}y, \quad \mathbf{u}(x, y) = \frac{1}{2\pi}\int_{-\infty}^{\infty} \mathrm{e}^{\mathrm{i}ky}\, \hat{\mathbf{u}}(x, k)\, \mathrm{d}k. \tag{3}$$

Theorem 1 (Convergence factor of the classical Schwarz algorithm)
For a given initial guess ($\mathbf{u}_1^0 \in (L^2(\Omega_1)^2)$, ($\mathbf{u}_2^0 \in (L^2(\Omega_2)^2)$, each Fourier mode k in the classical Schwarz algorithm (2) *converges with the corresponding convergence factor*

$$\rho_{cla}\left(k, \omega, C_p, C_s, \delta\right) = \max\{|r_+|, |r_-|\},$$

where

$$r_\pm = \frac{X^2}{2} + e^{-\delta(\lambda_1+\lambda_2)} \pm \frac{1}{2}\sqrt{X^2\left(X^2 + 4e^{-\delta(\lambda_1+\lambda_2)}\right)},\ X = \frac{k^2 + \lambda_1\lambda_2}{k^2 - \lambda_1\lambda_2}\left(e^{-\lambda_1\delta} - e^{-\lambda_2\delta}\right). \tag{4}$$

Here, $\lambda_{1,2} \in \mathbb{C}$ are the roots of the characteristic equation of the Fourier transformed Navier equations,

$$\lambda_1 = \sqrt{k^2 - \frac{\omega^2}{C_s^2}}, \quad \lambda_2 = \sqrt{k^2 - \frac{\omega^2}{C_p^2}}, \quad C_p = \sqrt{\frac{\lambda+2\mu}{\rho}}, \quad C_s = \sqrt{\frac{\mu}{\rho}}. \tag{5}$$

Proof By linearity it suffices to consider only the case $\mathbf{f} = 0$ and analyze convergence to the zero solution, see for example [9]. After a Fourier transform in the y direction, (1) becomes

$$\begin{cases} \left[(\lambda + 2\mu)\,\partial_x^2 + \left(\rho\omega^2 - \mu k^2\right)\right] \hat{u}_x + ik(\mu + \lambda)\partial_x \hat{u}_z = 0, \\ \left[\mu\partial_x^2 + \left(\rho\omega^2 - (\lambda + 2\mu)\,k^2\right)\right] \hat{u}_z + ik\,(\mu + \lambda)\,\partial_x \hat{u}_x = 0. \end{cases} \tag{6}$$

This is a system of ordinary differential equations, whose solution is obtained by computing the roots r of its characteristic equation,

$$\begin{bmatrix} (\lambda + 2\mu)r^2 + \rho\omega^2 - \mu k^2 & ik(\mu + \lambda)r \\ ik(\mu + \lambda)r & \mu r^2 + \rho\omega^2 - (\lambda + 2\mu)k^2 \end{bmatrix} \begin{bmatrix} \hat{u}_x \\ \hat{u}_z \end{bmatrix} = 0. \tag{7}$$

A direct computation shows that these roots are $\pm\lambda_1$ and $\pm\lambda_2$ where $\lambda_{1,2}$ are given by (5). Therefore the general form of the solution is

$$\hat{\mathbf{u}}(x,k) = \alpha_1 \mathbf{v}_+ e^{\lambda_1 x} + \beta_1 \mathbf{v}_- e^{-\lambda_1 x} + \alpha_2 \mathbf{w}_+ e^{\lambda_2 x} + \beta_2 \mathbf{w}_- e^{-\lambda_2 x}, \tag{8}$$

where $\mathbf{v}_\pm$ and $\mathbf{w}_\pm$ are obtained by successively inserting these roots into (7) and computing a non-trivial solution,

$$\mathbf{v}+ = \begin{pmatrix} 1 \\ \frac{\mathrm{i}\lambda_1}{k} \end{pmatrix}, \quad \mathbf{v}_- = \begin{pmatrix} 1 \\ -\frac{\mathrm{i}\lambda_1}{k} \end{pmatrix}, \quad \mathbf{w}_+ = \begin{pmatrix} -\frac{\mathrm{i}\lambda_2}{k} \\ 1 \end{pmatrix}, \quad \mathbf{w}_- = \begin{pmatrix} \frac{\mathrm{i}\lambda_2}{k} \\ 1 \end{pmatrix}. \tag{9}$$

Because the local solutions must remain bounded and outgoing at infinity, the subdomain solutions in the Fourier transformed domain are

$$\hat{\mathbf{u}}_1(x,k) = \alpha_1 \mathbf{v}_+ e^{\lambda_1 x} + \alpha_2 \mathbf{w}_+ e^{\lambda_2 x}, \qquad \hat{\mathbf{u}}_2(x,k) = \beta_1 \mathbf{v}_- e^{-\lambda_1 x} + \beta_2 \mathbf{w}_- e^{-\lambda_2 x}. \tag{10}$$

The coefficients $\alpha_{1,2}$ and $\beta_{1,2}$ are then uniquely determined by the transmission conditions. Before using the iteration to determine them, we rewrite the local solutions at iteration n in the form

$$\begin{aligned} \hat{\mathbf{u}}_1^n &= \alpha_1^n \mathbf{v}_+ e^{\lambda_1 x} + \alpha_2^n \mathbf{w}_+ e^{\lambda_2 x} = \begin{bmatrix} \mathrm{e}^{\lambda_1 x} & -\frac{i\lambda_2}{k}\,\mathrm{e}^{\lambda_2 x} \\ \frac{i\lambda_1}{k}\,\mathrm{e}^{\lambda_1 x} & \mathrm{e}^{\lambda_2 x} \end{bmatrix} \begin{pmatrix} \alpha_1^n \\ \alpha_2^n \end{pmatrix} =: M_x \boldsymbol{\alpha}^n, \\ \hat{\mathbf{u}}_2^n &= \beta_1^n \mathbf{v}_- e^{-\lambda_1 x} + \beta_2^n \mathbf{w}_- e^{-\lambda_2 x} = \begin{bmatrix} \mathrm{e}^{-\lambda_1 x} & \frac{i\lambda_2}{k}\,\mathrm{e}^{-\lambda_2 x} \\ -\frac{i\lambda_1}{k}\,\mathrm{e}^{-\lambda_1 x} & \mathrm{e}^{-\lambda_2 x} \end{bmatrix} \begin{pmatrix} \beta_1^n \\ \beta_2^n \end{pmatrix} =: N_x \boldsymbol{\beta}^n. \end{aligned} \tag{11}$$

We then insert (11) into the interface iteration of the classical Schwarz algorithm (2),

$$M_\delta \boldsymbol{\alpha}^n = N_\delta \boldsymbol{\beta}^{n-1} \;\Leftrightarrow\; \boldsymbol{\alpha}^n = M_\delta^{-1} N_\delta \boldsymbol{\beta}^{n-1}, \quad N_0 \boldsymbol{\beta}^n = M_0 \boldsymbol{\alpha}^{n-1} \;\Leftrightarrow\; \boldsymbol{\beta}^n = N_0^{-1} M_0 \boldsymbol{\alpha}^{n-1}.$$

This leads over a double iteration to

$$\boldsymbol{\alpha}^{n+1} = (M_\delta^{-1} N_\delta N_0^{-1} M_0)\boldsymbol{\alpha}^{n-1} =: R_\delta^1 \boldsymbol{\alpha}^{n-1}, \quad \boldsymbol{\beta}^{n+1} = (N_0^{-1} M_0 M_\delta^{-1} N_\delta)\boldsymbol{\beta}^{n-1} =: R_\delta^2 \boldsymbol{\beta}^{n-1},$$

where $R_\delta^{1,2}$ are the iteration matrices which are spectrally equivalent. The iteration matrix R_δ^1 is given by

$$R_\delta^1 = \begin{bmatrix} e^{-\delta(\lambda_1+\lambda_2)} X_2^2 \frac{\lambda_1}{\lambda_2} + e^{-2\lambda_1\delta} X_1^2 & X_1 X_2 \left(e^{-2\lambda_1\delta} - e^{-\delta(\lambda_1+\lambda_2)}\right) \\ X_1 X_2 \frac{\lambda_1}{\lambda_2} \left(e^{-\delta(\lambda_1+\lambda_2)} - e^{-2\lambda_2\delta}\right) & e^{-\delta(\lambda_1+\lambda_2)} X_2^2 \frac{\lambda_1}{\lambda_2} + e^{-2\lambda_2\delta} X_1^2 \end{bmatrix}, \tag{12}$$

where $X_1 = \frac{k^2+\lambda_1\lambda_2}{k^2-\lambda_1\lambda_2}$ and $X_2 = -i\frac{2k\lambda_2}{k^2-\lambda_1\lambda_2}$. A direct computation then leads to the eigenvalues (r_+, r_-) of R_δ^1,

$$r_\pm = \frac{X^2}{2} + e^{-\delta(\lambda_1+\lambda_2)} \pm \frac{1}{2}\sqrt{X^2\left(X^2 + 4e^{-\delta(\lambda_1+\lambda_2)}\right)}, \quad X = \frac{k^2+\lambda_1\lambda_2}{k^2-\lambda_1\lambda_2}\left(e^{-\lambda_1\delta} - e^{-\lambda_2\delta}\right). \tag{13}$$

The convergence factor is given by the spectral radius of the matrix $R_\delta^{1,2}$,

$$\rho_{cla}\left(k, \omega, C_p, C_s, \delta\right) = \max\{|r_+|, |r_-|\}, \tag{14}$$

which concludes the proof. □

Corollary 1 (Classical Schwarz without Overlap)

In the case without overlap, $\delta = 0$, we obtain from (4) that $r_\pm = 1$, since $\left(R_\delta^1 = \mathrm{Id}\right)$. Therefore, the classical Schwarz algorithm is not convergent without overlap, it just stagnates.

The result in Corollary 1 is consistent with the general experience that Schwarz methods without overlap do not converge, but there are important exceptions, for example for hyperbolic problems [4], and also optimized Schwarz methods can converge without overlap [9]. Unfortunately also with overlap, the Schwarz method has difficulties with the time harmonic Navier equations (1):

Corollary 2 (Classical Schwarz with Overlap)

The convergence factor of the overlapping classical Schwarz method (2) with overlap δ applied to the Navier equations (1) verifies for δ small enough

$$\rho_{cla}\left(k, \omega, C_p, C_s, \delta\right) \begin{cases} = 1, \ k \in [0, \frac{\omega}{C_p}] \cup \{\frac{\omega}{C_s}\}, \\ > 1, \ k \in (\frac{\omega}{C_p}, \frac{\omega}{C_s}), \\ < 1, \ k \in (\frac{\omega}{C_s}, \infty). \end{cases}$$

It thus converges only for high frequencies, diverges for medium frequencies, and stagnates for low frequencies.

Proof We only give here the outline of the proof, the details will appear in [2], see also [1]: for the first interval $k \in [0, \frac{\omega}{C_p})$, the proof is obtained by a direct, but long and technical calculation. For the second and third interval, $k \in (\frac{\omega}{C_p}, \frac{\omega}{C_s})$ and $k \in (\frac{\omega}{C_s}, \infty)$, we compute the modulus of the eigenvalues and expand them for δ small to obtain the result. At the boundary between those intervals for $k \in \{\frac{\omega}{C_p}, \frac{\omega}{C_s}\}$,

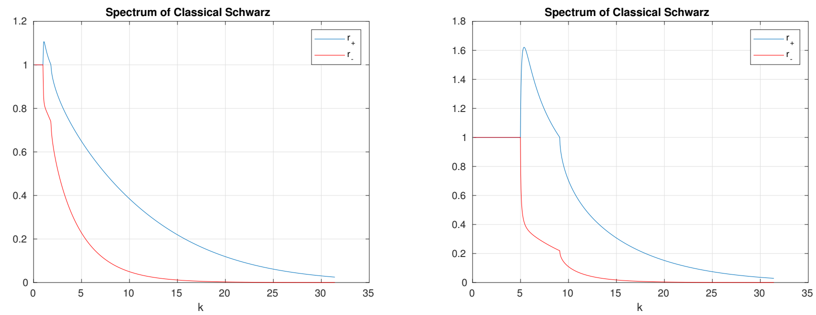

Fig. 1 Modulus of the eigenvalues of the iteration matrix as a function of Fourier frequency for the classical Schwarz method with $C_p = 1$, $C_s = 0.5$, $\rho = 1$, $\delta = 0.1$. Left: for $\omega = 1$. Right: for $\omega = 5$.

the natural simplifications $\lambda_2 = 0$ or $\lambda_1 = 0$ lead directly to the result[2]. We illustrate the three zones of different convergence behavior for two examples in Figure 1.

We see from Corollary 2 that the classical Schwarz method with overlap can not be used as an iterative solver to solve the time harmonic Navier equations, since it is in general divergent on the whole interval of intermediate frequencies $(\frac{\omega}{C_p}, \frac{\omega}{Cs})$. This is even worse than for the Helmholtz or Maxwell's equations where the overlapping classical Schwarz algorithm is also convergent for high frequencies, and only stagnates for low frequencies, but is never divergent. A precise estimate of how fast the classical Schwarz method applied to the time harmonic Navier equations diverges depending on the overlap is given by the following theorem:

Theorem 2 (Asymptotic convergence factor)
The maximum of the convergence factor of the classical Schwarz method (2) applied to the Navier equations (1) behaves for small overlap δ asymptotically as

$$\max_k(\max|r_\pm|) \sim 1 + \frac{\sqrt{2}C_s\omega\left(3C_p^2-\sqrt{C_p^4+8C_s^4}\right)\sqrt{C_p^2\sqrt{C_p^4+8C_s^4}-C_p^4-2C_s^4}}{C_p(C_p^2+C_s^2)^{\frac{3}{2}}\left(\sqrt{C_p^4+8C_s^4}-C_p^2\right)}\delta.$$

Proof According to Corollary 2, the maximum of the convergence factor is attained in the interval where the algorithm is divergent, $k \in (\frac{\omega}{C_p}, \frac{\omega}{C_s})$, and this quantity is larger than one. For a fixed k and a small overlap δ, the convergence factor $\rho_{cla}(k, \omega, C_p, C_s, \delta)$ for $k \in (\frac{\omega}{C_p}, \frac{\omega}{C_s})$ is given by

$$\rho_{cla}(k, \omega, C_p, C_s, \delta) = 1 + \frac{2\omega^2\lambda_2\bar{\lambda}_1^2}{C_p^2\left(k^4+\bar{\lambda}_1^2\lambda_2^2\right)}\delta + O\left(\delta^2\right) \in \mathbb{R}_+^*. \quad (15)$$

[2] The two values $k = \frac{\omega}{C_p}$ and $k = \frac{\omega}{C_s}$ correspond to points in the spectrum where the underlying Navier equations are singular, and are similar to the one resonance frequency in the Helmholtz case. They are avoided in practice either by using radiation boundary conditions on parts of the boundary of the computational domain, or by choosing domain geometries such that these frequencies are not part of the discrete spectrum of the Navier operator on the bounded domain.

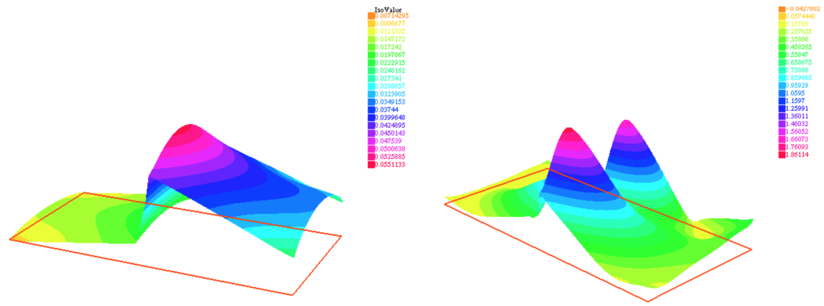

Fig. 2 Error in modulus at iteration 25 of the classical Schwarz method with 2 subdomains, where one can clearly identify the dominant mode in the error: Left: $\omega = 1$. Right: $\omega = 5$.

We denote by $C(k)$ the coefficient in front of δ. In order to compute the maximum of (15) we solve the equation $\frac{dC(k)}{dk} = 0$. We denote by k_s the only positive critical point for which $\frac{d^2C(k)}{dk^2}(k_s) < 0$. By replacing k_s into the expression of $C(k)$ we get the desired result, see [1] for more details. □

3 Numerical experiments

We illustrate now the divergence of the classical Schwarz algorithm with a numerical experiment. We choose the same parameters $C_p = 1$, $C_s = 0.5$, $\rho = 1$ and overlap $\delta = 0.1$ as in Figure 1. We discretize the time-harmonic Navier equations using $P1$ finite elements on the domain $\Omega = (-1, 1) \times (0, 1)$ and impose absorbing boundary conditions on $\partial\Omega$. We decompose the domain into two overlapping subdomains $\Omega_1 = (-1, 2h) \times (0, 1)$ and $\Omega_2 = (-2h, 1) \times (0, 1)$ with $h = \frac{1}{40}$, such that the overlap $\delta = 0.1 = 4h$. Our computations are performed with the open source software Freefem++. We show in Figure 2 the error in modulus at iteration 25 of the classical Schwarz method, on the left for $\omega = 1$ and on the right for $\omega = 5$. In the first case, $\omega = 1$, we observe very slow convergence, the error decreases from $7.89e-1$ to $5e-2$ after 25 iterations. This can be understood as follows: the lowest frequency along the interface on our domain Ω is $k = \pi$, which lies outside the interval $[\frac{\omega}{C_p}, \frac{\omega}{C_s}] = [1, 2]$ of frequencies on which the method is divergent. The method thus converges, all frequencies lie in the convergent zone in the plot in Figure 1 on the left where $\rho_{cla} < 1$. The most slowly convergent mode is $|\sin(ky)|$ with $k = \pi$, which is clearly visible in Figure 2 on the left. This is different for $\omega = 5$, where we see in Figure 2 on the right the dominant growing mode. The interval of frequencies on which the method is divergent is given by $[\frac{\omega}{C_p}, \frac{\omega}{C_s}] = [5, 10]$, and we clearly can identify in Figure 2 on the right a mode with two bumps along the interface, which corresponds to the mode $|\sin(ky)|$ along the interface for $k = 2\pi \approx 6$, which is the

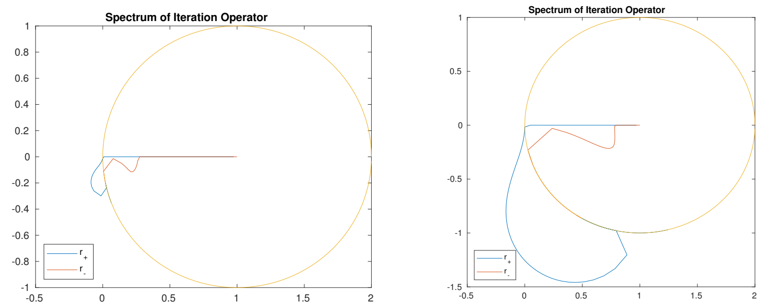

Fig. 3 Spectrum of the iteration operator for the same example as in Figure 1, together with a unit circle centered around the point $(1, 0)$. Left: $\omega = 1$. Right: $\omega = 5$

fastest diverging mode according to the analytical result shown in Figure 1 on the right.

One might wonder if the classical Schwarz method is nevertheless a good preconditioner for a Krylov method, which can happen also for divergent stationary methods, like for example the Additive Schwarz Method applied to the Laplace problem, which is also not convergent as an iterative method [6], but useful as a preconditioner. To investigate this, it suffices to plot the spectrum of the identity matrix minus the iteration operator in the complex plane, which corresponds to the preconditioned systems one would like to solve. We see in Figure 3 that the part of the spectrum that leads to a contraction factor ρ_{cla} with modulus bigger than one lies unfortunately close to zero in the complex plane, and that is where the residual polynomial of the Krylov method must equal one. Therefore we can infer that the classical Schwarz method will also not work well as a preconditioner. This is also confirmed by the numerical results shown in Figure 4, where we used first the classical Schwarz method as a solver and then as preconditioner for GMRES. We see that GMRES now makes the method converge, but convergence depends strongly on ω and slows down when ω grows.

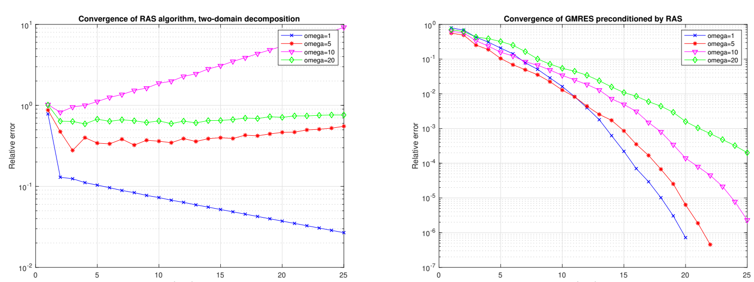

Fig. 4 Convergence history for RAS and GMRES preconditioned by RAS for different values of ω

4 Conclusion

We proved that the classical Schwarz method with overlap applied to the time harmonic Navier equations cannot be used as an iterative solver, since it is not convergent in general. This is even worse than for the Helmholtz or time harmonic Maxwell's equations, for which the classical Schwarz algorithm also stagnates for all propagative modes, but at least is not divergent. We then showed that our analysis clearly identifies the problematic error modes in a numerical experiment. Using the classical Schwarz method as a preconditioner for GMRES then leads to a convergent method, which however is strongly dependent on the time-harmonic frequency parameter ω. We are currently studying better transmission conditions between subdomains, which will lead to optimized Schwarz methods for the time harmonic Navier equation.

References

1. R. Brunet. Domain decomposition methods for time-harmonic elastic waves. *PhD thesis, University of Strathclyde*, 2018.
2. R. Brunet, V. Dolean, M.J. Gander. Natural domain decomposition algorithtms for the solution of time-harmonic elastic waves. *paper in preparation*.
3. O. Darrigol. Between hydrodynamics and elasticity theory: the first five births of the Navier-Stokes equation. *Archive for History of Exact Sciences, Springer*, 56(2):95–150, 2002.
4. V. Dolean and M.J. Gander. Why Classical Schwarz Methods Applied to Hyperbolic Systems Can Converge even Without Overlap. *Domain decomposition methods in science and engineering XVII*, Springer, 467–475, 2008.
5. V. Dolean, M.J. Gander, and L. Gerardo-Giorda. Optimized Schwarz methods for Maxwell's equations. *SIAM J. Sci. Comput.*, vol 31, pp. 2193-2213, 2009.
6. E. Efstathiou and M.J. Gander. Why restricted additive Schwarz converges faster than additive Schwarz. *BIT. Numerical Mathematics*, vol 43, pp. 945-959, 2003.
7. A.C. Eringen, and E.S. Suhubi, Elastodynamics, Vol. 2. *ACADEMIC PRESS New York San Francisco London*, 1977.
8. O.G. Ernst, M.J. Gander. Why it is difficult to solve Helmholtz problems with classical iterative methods. *Numerical analysis of multiscale problems, Springer*, pp. 325-363, 2012.
9. M.J. Gander. Optimized Schwarz methods. *SIAM Journal on Numerical Analysis*, 44(2):699–731, 2006.
10. T. Huttunen, P. Monk, F. Collino, and P. Kaipio Jari. The ultra-weak variational formulation for elastic wave problems. *SIAM Journal on Scientific Computing*, 25(5):1717–1742, 2004.
11. B. Lautrup. Physics of continuous matter: exotic and everyday phenomena in the macroscopic world. *CRC press*, 2011.